Stem Cell Reports
Report
ISSCR
OPEN ACCESS

A CRISPR/Cas9-Based System for Reprogramming Cell Lineage Specification

Syandan Chakraborty,[1,5] HaYeun Ji,[1,5] Ami M. Kabadi,[1] Charles A. Gersbach,[1,2,3] Nicolas Christoforou,[1,4] and Kam W. Leong[1,5,*]
[1]Department of Biomedical Engineering, Duke University, Durham, NC 27708, USA
[2]Institute for Genome Sciences and Policy, Duke University, Durham, NC 27708, USA
[3]Department of Orthopaedic Surgery, Duke University Medical Center, Durham, NC 27708, USA
[4]Department of Biomedical Engineering, Khalifa University, Abu Dhabi 127788, UAE
[5]Department of Biomedical Engineering, Columbia University, New York, NY 10027, USA
*Correspondence: kam.leong@duke.edu
http://dx.doi.org/10.1016/j.stemcr.2014.09.013

SUMMARY

Gene activation by the CRISPR/Cas9 system has the potential to enable new approaches to science and medicine, but the technology must be enhanced to robustly control cell behavior. We show that the fusion of two transactivation domains to Cas9 dramatically enhances gene activation to a level that is necessary to reprogram cell phenotype. Targeted activation of the endogenous *Myod1* gene locus with this system led to stable and sustained reprogramming of mouse embryonic fibroblasts into skeletal myocytes. The levels of myogenic marker expression obtained by the activation of endogenous *Myod1* gene were comparable to that achieved by overexpression of lentivirally delivered MYOD1 transcription factor.

INTRODUCTION

The type II clustered regularly interspaced short palindromic repeat (CRISPR) systems and the associated Cas9 nucleases have evolved in archaea and bacteria for sequence-specific recognition of DNA targets via a single-stranded RNA intermediate (Jinek et al., 2012). In an engineered version of the CRISPR system, the *Streptococcus pyogenes* Cas9 nuclease is directed by guide RNAs (gRNAs) targeting 20 bp sequences adjacent to a 5′-NRG-3′ sequence motif, and the resultant cleavage has been used to edit the genome in several species (Cho et al., 2013; Cong et al., 2013; Hwang et al., 2013; Jinek et al., 2013; Mali et al., 2013b). A mutated nuclease-inactive Cas9 (dCas9) regulates gene expression by physically blocking transcription or through fusion to a transactivator (VP64, Ω subunit of RNA polymerase) or repressor domain (KRAB, SID) (Bikard et al., 2013; Cheng et al., 2013; Farzadfard et al., 2013; Gilbert et al., 2013; Kearns et al., 2014; Konermann et al., 2013; Maeder et al., 2013; Mali et al., 2013a; Perez-Pinera et al., 2013; Qi et al., 2013). While transgene overexpression has been used to achieve cellular reprogramming (Davis et al., 1987; Takahashi and Yamanaka, 2006), reprogramming via direct activation of an endogenous gene has only been recently demonstrated through the use of transcription activator-like effectors (TALEs) (Gao et al., 2013). However, difficulty in designing and codelivering multiple TALE expression constructs precludes simple screening and multiplexed gene activation that is straightforward with the dCas9-VP64 system. In this study, we used dCas9-based transactivators combined with an efficient lentivirus-based gene delivery system to induce cellular reprogramming.

RESULTS AND DISCUSSION

We tested the efficacy of a ^{VP64}dCas9-BFP^{VP64} fusion protein to activate expression of the endogenous *Myod1* gene locus for a sufficient duration and magnitude to ultimately induce the reprogramming of mouse embryonic fibroblasts (MEFs) to skeletal myocytes (SkMs) (Figure 1A). Although we and others have previously used the single C-terminal fusion of VP64 to dCas9 to activate gene expression (Cheng et al., 2013; Farzadfard et al., 2013; Gilbert et al., 2013; Kabadi et al., 2014; Maeder et al., 2013; Perez-Pinera et al., 2013), preliminary studies indicated that this approach did not lead to levels of expression sufficient for cell reprogramming. Therefore, we tested whether two VP64 domains flanking dCas9 (^{VP64}dCas9-BFP^{VP64}) would yield higher *Myod1* gene expression levels (Figures 1B and 1C and Figure S1A available online). dCas9 was also fused to blue fluorescent protein (BFP) to monitor expression (Figures 1B, 1C, S1A, and S1B). Lentiviral ^{VP64}dCas9-BFP^{VP64} was placed under the transcriptional control of a doxycycline-inducible promoter (Figures 1C and S1B). To avoid steric hindrance that may prevent transcriptional complex recruitment, we included flexible glycine-serine linkers adjacent to the VP64 domains (Figure S1A). We also added a third nuclear localization signal (NLS), which improved the nuclear localization of ^{VP64}dCas9-BFP^{VP64} by ~10-fold (Figures 1C–1F). Initially, we transfected C3H10T1/2 cells with the ^{VP64}dCas9-BFP^{VP64} plasmid. However, transfection was inefficient as transgene expression was detectable only in a few cells, presumably due to the large size of the plasmid (13.5 kb). We then used a lentiviral gene delivery system, allowing stable transduction of more cells as

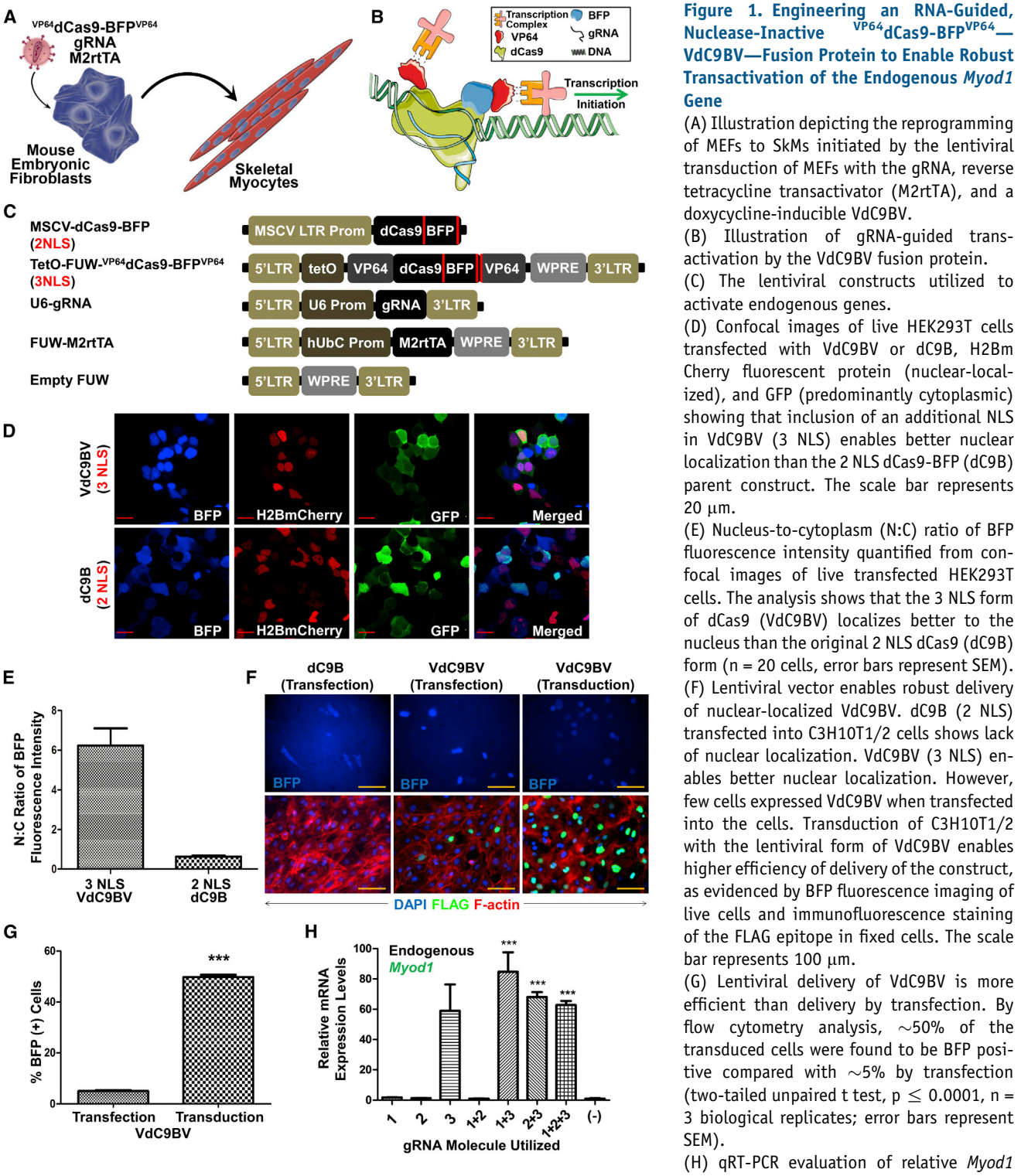

Figure 1. Engineering an RNA-Guided, Nuclease-Inactive ^{VP64}dCas9-BFP^{VP64}—VdC9BV—Fusion Protein to Enable Robust Transactivation of the Endogenous *Myod1* Gene

(A) Illustration depicting the reprogramming of MEFs to SkMs initiated by the lentiviral transduction of MEFs with the gRNA, reverse tetracycline transactivator (M2rtTA), and a doxycycline-inducible VdC9BV.

(B) Illustration of gRNA-guided transactivation by the VdC9BV fusion protein.

(C) The lentiviral constructs utilized to activate endogenous genes.

(D) Confocal images of live HEK293T cells transfected with VdC9BV or dC9B, H2Bm Cherry fluorescent protein (nuclear-localized), and GFP (predominantly cytoplasmic) showing that inclusion of an additional NLS in VdC9BV (3 NLS) enables better nuclear localization than the 2 NLS dCas9-BFP (dC9B) parent construct. The scale bar represents 20 μm.

(E) Nucleus-to-cytoplasm (N:C) ratio of BFP fluorescence intensity quantified from confocal images of live transfected HEK293T cells. The analysis shows that the 3 NLS form of dCas9 (VdC9BV) localizes better to the nucleus than the original 2 NLS dCas9 (dC9B) form (n = 20 cells, error bars represent SEM).

(F) Lentiviral vector enables robust delivery of nuclear-localized VdC9BV. dC9B (2 NLS) transfected into C3H10T1/2 cells shows lack of nuclear localization. VdC9BV (3 NLS) enables better nuclear localization. However, few cells expressed VdC9BV when transfected into the cells. Transduction of C3H10T1/2 with the lentiviral form of VdC9BV enables higher efficiency of delivery of the construct, as evidenced by BFP fluorescence imaging of live cells and immunofluorescence staining of the FLAG epitope in fixed cells. The scale bar represents 100 μm.

(G) Lentiviral delivery of VdC9BV is more efficient than delivery by transfection. By flow cytometry analysis, ~50% of the transduced cells were found to be BFP positive compared with ~5% by transfection (two-tailed unpaired t test, $p \leq 0.0001$, n = 3 biological replicates; error bars represent SEM).

(H) qRT-PCR evaluation of relative *Myod1* mRNA expression in C3H10T1/2 on day 6 postinduction of VdC9BV expression in the presence of various combinations of three gRNA molecules ($p \leq 0.001$, one-way ANOVA, Dunnett's post hoc comparing all the groups to the [−] gRNA control group [M2rtTA + VdC9BV + Empty FUW], n = 3 biological replicates, error bars represent SEM).

evidenced by both BFP and immunofluorescence staining of the FLAG epitope (Figure 1F). Approximately 50% of the transduced cells were found to be BFP positive as compared with 5% by transfection (Figure 1G). To ensure efficient gRNA codelivery, we developed a lentivirus-based U6 promoter-driven gRNA delivery system (Figure 1C). In separate experiments, we observed an ~6-fold upregulation of *Myod1* mRNA levels when all components were delivered by transfection (Figure S1C) compared with ~60-fold by lentiviral transduction (Figure 1H).

We initially tested this system's capacity to induce epigenetic reprogramming toward the SkM lineage in C3H10T1/2 cells previously shown to readily undergo this transformation (Davis et al., 1987). We designed three separate gRNAs (1–3) targeted to different positions proximal to the *Myod1* transcription start site and initially codelivered all three gRNAs (Figure S1D). We found that VP64 fusion and the presence of the gRNA were essential for endogenous *Myod1* gene activation (Figure S1C). Activation of the endogenous *Myod1* gene in C3H10T1/2 was sufficient to initiate the SkM reprogramming process, as determined by gene expression analysis, phase contrast imaging, and immunocytochemistry (Figures 2A–2C and S1B). Myotubes were visible as early as 4.5 days after transduction. Nuclear-localized blue fluorescence was observed in the myotubes during the time ^{VP64}dCas9-BFP^{VP64} was kept induced by doxycycline addition (Figure S1B). Importantly, the myotubes stained positive for the skeletal transcription factors (TFs) MYOD1 and MYOG, and the sarcomeric proteins actinin, desmin, myosin heavy chain, and titin (Figures 2C and S2A). The myotubes were also multinucleated, indicating cell fusion, one of the hallmarks of myogenic reprogramming (Figure 2C). When examining the effect of individual gRNA molecules in inducing *Myod1* mRNA expression, we determined that gRNA3 alone was as potent as all three gRNAs combined (Figure 1H). We speculate that factors, including distance from transcription initiation site, low binding affinity, and binding site competition with endogenous TFs, are the possible causes of gRNA1 and gRNA2 inactivity. C3H10T1/2 cells fused in the 8 days that *Myod1* was expressed under doxycycline-induced ^{VP64}dCas9-BFP^{VP64} expression, as demonstrated quantitatively by a recombination-based cell fusion assay. The fusion process continued unabated even after the withdrawal of doxycycline, thereby indicating stability of this phenotypic transformation (Figure 2D).

We tested whether coexpression of a single targeting gRNA molecule (gRNA3) along with ^{VP64}dCas9-BFP^{VP64} would be sufficient to induce reprogramming of primary MEFs (Figure 2E). Using gene expression analysis, we readily detected transcriptional activation of the mature myotube markers *Myl1*, *Ckm*, *Desmin*, and *Chrna1* (Figure 2F). We detected formation of multinucleated myotubes expressing skeletal TFs and striated sarcomeres indicating a high degree of cytoskeletal organization and maturity (Figures 2G and S2B). Within 3 weeks of cell transduction, we observed myotubes exhibiting spontaneous intermittent twitching (Movie S1).

To test whether transient expression of ^{VP64}dCas9-BFP^{VP64} is sufficient to induce sustained expression of *Myod1*, we induced transgene expression between days 2 and 10 posttransduction. We detected an initial robust upregulation of ^{VP64}dCas9-BFP^{VP64} expression followed by a gradual downregulation suggesting transgene silencing in the reprogramming cells (Figure 3A). Doxycycline removal coincided with rapid ^{VP64}dCas9-BFP^{VP64} decline to levels measured prior to initial induction. ^{VP64}dCas9-BFP^{VP64} expression also coincided with an increase in *Myod1* expression. Importantly, *Myod1* mRNA levels remained elevated for the duration of the 18-day experiment even after doxycycline removal (day 10), suggesting that maintenance of endogenous activation of *Myod1* is stable and independent of ^{VP64}dCas9-BFP^{VP64} activity.

dCas9 with VP64 fused to its C terminus (dCas9-BFP^{VP64}) failed to activate the *Myod1* locus to levels sufficient to initiate cellular reprogramming even in the presence of three gRNAs (Figures 3B, 3C, and S3A). However, in the presence of three gRNAs, the mean fold-activation level by dCas9-BFP^{VP64} was higher than with a single gRNA (Figure 3C), consistent with recent reports of synergistic effects of multiple gRNAs with dCas9 and a single VP64 fusion (Cheng et al., 2013; Maeder et al., 2013; Mali et al., 2013a; Perez-Pinera et al., 2013). The N-terminal-only VP64 fusion protein (^{VP64}dCas9-BFP) also failed to match the ability of ^{VP64}dCas9-BFP^{VP64} to activate sufficient endogenous *Myod1* for reprogramming in the presence of a single gRNA (Figures 3B, 3D, and S3A). Interestingly, ^{VP64}dCas9-BFP^{VP64} was able to activate the endogenous human *MYOD1* locus significantly in the presence of a single gRNA, whereas the N-terminal-only VP64 fusion protein (^{VP64}dCas9-BFP) and the C-terminal-only VP64 fusion protein (dCas9-BFP^{VP64}) failed to do so (Figure 3E). These observations suggest that the inclusion of both VP64 activator domains fused at the two termini of dCas9-BFP significantly improves the activation capacity of this targeting platform. However, the endogenous human *MYOD1* transactivation was an order of magnitude lower than that observed in the murine system. Transactivation of higher levels of *MYOD1* mRNA may require extensive optimization of the gRNA target sequences in the future.

To test whether the direction of the genomic strand targeted by the gRNA molecule was a factor in its capacity to recruit dCas9 and activate expression of the endogenous locus, we designed a gRNA molecule (gRNA4) targeting the minus strand of the same region for which gRNA3 was

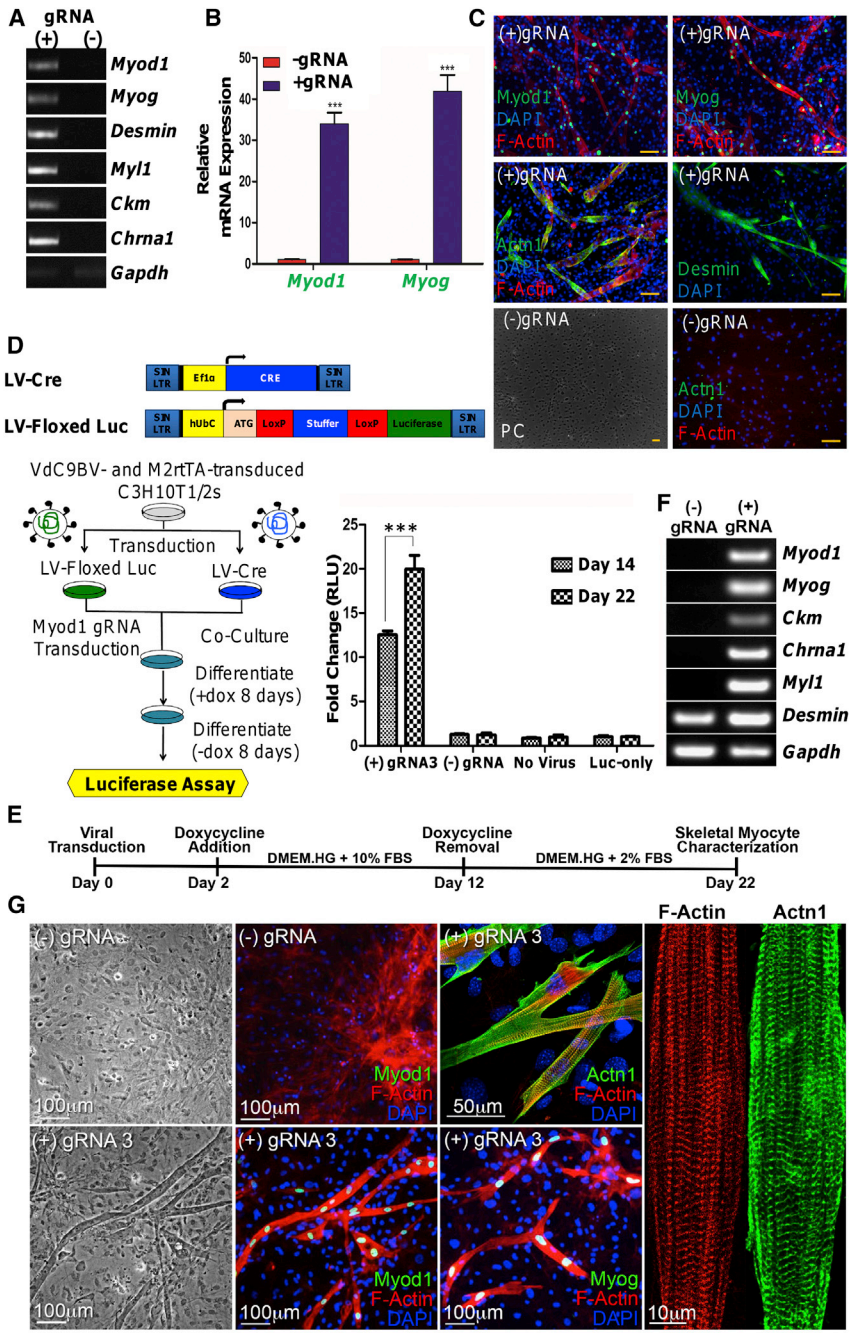

Figure 2. CRISPR/^{VP64}dCas9-BFP^{VP64} Transactivates the Endogenous *Myod1* Gene and Reprograms C3H10T1/2 Cells and MEFs into SkMs

(A) ^{VP64}dCas9-BFP^{VP64} (VdC9BV), in the presence of three gRNAs targeting the *Myod1* locus, results in upregulation of major SkM genes in C3H10T1/2 cells detected by RT-PCR on day 18 posttransduction.

(B) Reprogramming of C3H10T1/2 cells by VdC9BV is characterized by significantly higher levels of *Myod1* and *Myog* mRNA detected by qRT-PCR on day 18 post-transduction (two-way ANOVA, Bonferroni post tests, $p \leq 0.001$ for both *Myod1* and *Myog*, n = 3 biological replicates, error bars represent SEM). Fold change in expression is relative to the (−) gRNA control group.

(C) Immunocytochemistry (ICC) of reprogrammed C3H10T1/2 cells for SkM markers. The multinucleated myotubes stained for nuclear MYOD1 and MYOG proteins and sarcomeric proteins desmin and ACTN1 (α-actinin). Reprogrammed myotubes were absent in the control group (phase contrast [PC] imaging and ICC). The scale bar represents 100 μm.

(D) Cell fusion assay. Cell fusion in the reprogramming cells was quantified by detecting the luciferase released after mixing two lentivirally transduced cell populations: one expressing Cre recombinase (LV-Cre) and a second containing a Cre recombinase responsive Floxed-Stuffer Luciferase cassette (LV-Floxed Luc). Fold change in relative light units (RLUs) was calculated relative to a Luc-only group (VdC9BV, M2rtTA, and LV-Floxed Luc). The RLU fold change of the (+) gRNA3 group is significantly higher on day 22 than on day 14 (two-way repeated measures [RM] ANOVA, Bonferroni post hoc test, $p \leq 0.001$, n = 3 biological replicates, error bars = SEM). Overall, the (+) gRNA3 group has significantly higher luciferase activity than other groups (two-way RM ANOVA, $p \leq 0.0001$).

(E) Timeline denoting the main steps of the MEF reprogramming process.

(F) Gene expression analysis (RT-PCR) performed on reprogrammed and control MEFs.

(G) Imaging of the reprogrammed MEFs shows the presence of multinucleated myotubes containing SkM markers. No myogenesis was observed in the (−) control group. Confocal imaging shows cross-striated organization of ACTN1 and F-actin.

designed (PAM separated by 14 bases) (Figure S1D). Interestingly, gRNA4 was also able to activate *Myod1* expression and initiate reprogramming, indicating the system is insensitive to the target strand (Figures 3F and S3B).

We also evaluated the effect of BFP fusion on the activity of ^{VP64}dCas9-BFP^{VP64}. Following transduction at equivalent multiplicity of infection (MOIs), the construct without BFP showed statistically higher levels of dCas9 expression, although it was less efficacious than the BFP-fused form in inducing expression of *Myod1* (Figures 3B and 3G). However, both forms led to reprogramming (Figure S3C). The omission of BFP from the C-terminal-only VP64 fusion

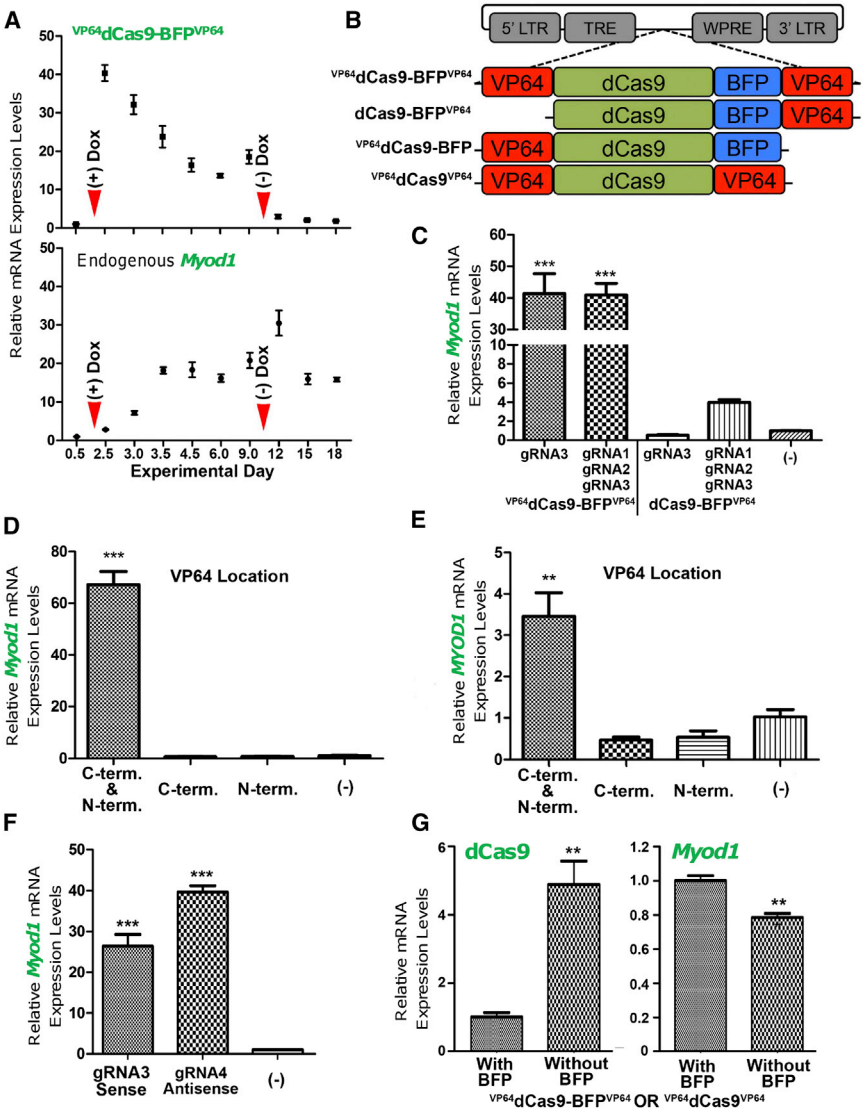

Figure 3. Characteristics of gRNA-Guided ^{VP64}dCas9-BFP^{VP64}-Mediated Activation of the Endogenous *Myod1* Gene Locus

(A) VdC9BV-mediated activation of the endogenous murine *Myod1* gene is stable and sustained following doxycycline removal. The red arrowheads indicate the time points on which addition and removal of doxycycline are performed. dCas9 expression kinetics is significantly different from that of transactivated *Myod1* ($p \leq 0.0001$, two-way ANOVA). Fold change in expression is relative to levels at day 0.5 posttransduction (n = 4 biological replicates, error bars represent SEM).

(B) Illustration of dCas9-based activators.

(C) The C-terminal-only fusion of VP64 to dCas9, dCas9-BFP^{VP64}, fails to activate the endogenous murine *Myod1* gene in C3H10T1/2 cells even in the presence of multiple gRNAs. VdC9BV significantly activated transcription of the endogenous *Myod1* gene locus when compared with all other groups ($p \leq 0.001$, one-way ANOVA, Tukey's post hoc test, n = 3). Control group: M2rtTA + Empty FUW. Fold change in expression is relative to the (−) control group.

(D) The N-terminal-only VP64 fusion to dCas9 (^{VP64}dCas9-BFP) also failed to match the ability of VdC9BV to transactivate significant levels of endogenous *Myod1* expression in the presence of a single gRNA ($p \leq 0.001$, one-way ANOVA, Dunnett's post hoc test, n = 3). Control: M2rtTA +Empty FUW. Fold change in expression is relative to the (−) control group.

(E) Only the N- and C-terminal VP64 fusion to dCas9 (VdC9BV) significantly activated the human *MYOD1* locus of HEK293T cells in the presence of a gRNA ($p \leq 0.01$, one-way ANOVA, Dunnett's post hoc test, n = 3).

(F) A gRNA targeting the antisense strand (gRNA4) can significantly activate endogenous *Myod1* expression to levels similar to that achieved by the gRNA targeting the sense strand (gRNA3) ($p \leq 0.001$, one-way ANOVA, Dunnett's post hoc comparing all the groups to the [−] gRNA group, n = 3). (−) gRNA group: M2rtTA + VdC9BV + Empty FUW virus. Fold change in expression is relative to the (−) control group.

(G) In the absence of the BFP domain, ^{VP64}dCas9^{VP64} activates *Myod1* expression to a lesser extent than the VdC9BV group, although dCas9 is expressed at a significantly higher level using the same MOI (C3H10T1/2 cells, unpaired two-tailed t test p = 0.0051 [dCas9], p = 0.0044 [*Myod1*], n = 3). Fold change in expression is relative to the VdC9BV group. Measurements for (C–G) occurred at posttransduction day 6, and the data from independent biological replicates are represented as mean ± SEM.

protein (dCas9^{VP64}) failed to impart ability to activate the endogenous *Myod1* locus (Figure S3D). We speculate that the positive effect of BFP on *Myod1* expression may be due to increased spacing between the two VP64 domains or increased flexibility of the domains.

We also compared the ^{VP64}dCas9-BFP^{VP64}-mediated activation of endogenous *Myod1* gene to transgenic MYOD1 overexpression for its ability to reprogram cells. C3H10T1/2 cells were transduced with ^{VP64}dCas9-BFP^{VP64} and M2rtTA. The resultant BFP-positive cells were sorted for BFP expression and the BFP^{+} cells were transduced with either gRNA or doxycycline-inducible transgenic human MYOD1 at equivalent MOIs (MOI = 10) (Figures 4A and 4B). During the induction phase of the reprogramming

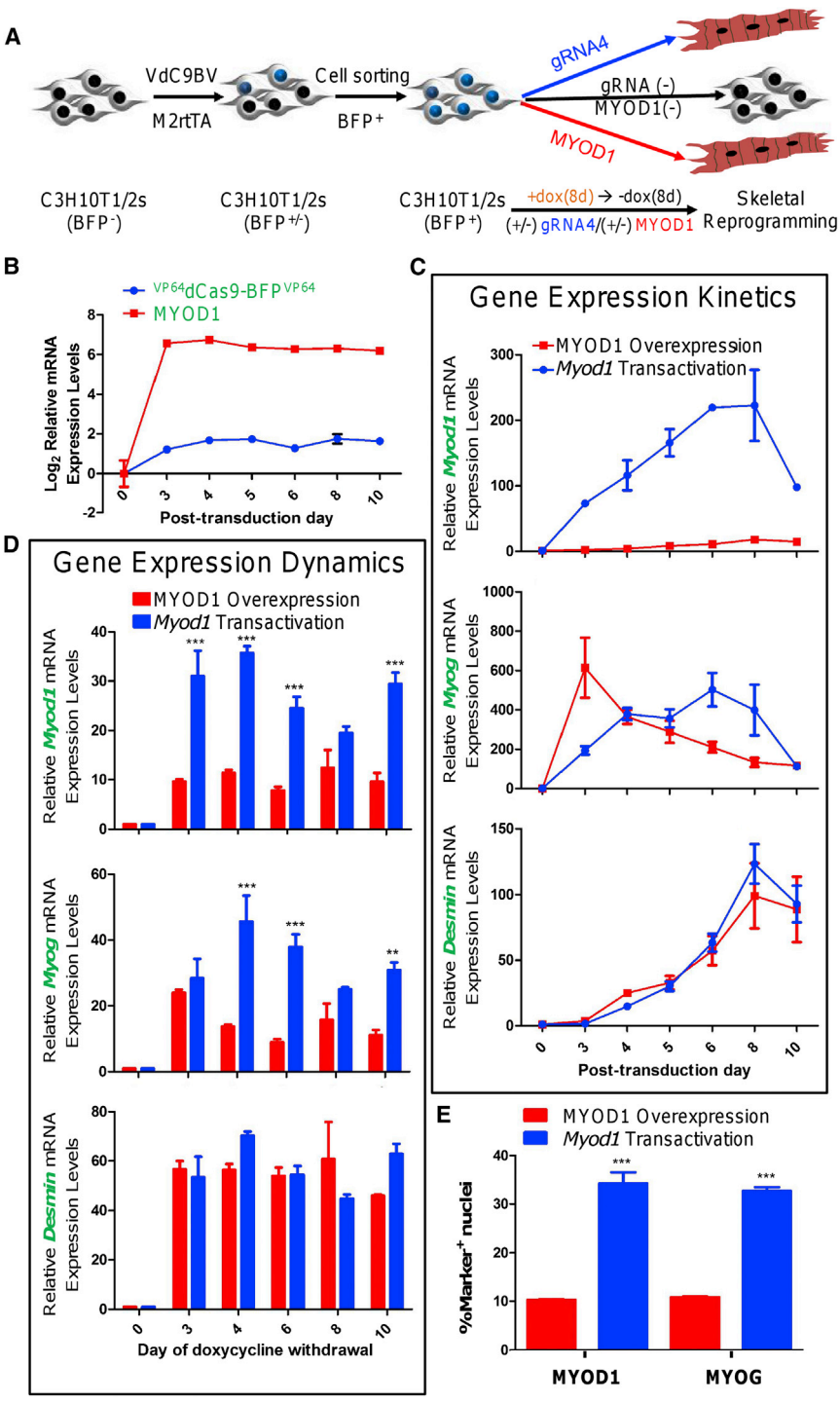

Figure 4. Comparison of Skeletal Reprogramming by gRNA-Guided ^{VP64}dCas9-BFP^{VP64}-Mediated Transactivation of the Endogenous *Myod1* Gene Locus and by Transgenic MYOD1 Overexpression

(A) Illustration depicting the experimental setup for the comparison of skeletal reprogramming by *Myod1* transactivation and by transgenic MYOD1 overexpression.

(B) Expression kinetics of VdC9BV and MYOD1 transgenes under doxycycline induction from days 2 to 10 posttransduction.

(C) Expression kinetics of myogenic genes (*Myod1*, *Myog*, and *Desmin*) in C3H10T1/2 cells detected by qRT-PCR during the 8 days of doxycycline induction of both the systems. The endogenous *Myod1* expression over the entire duration of induction is significantly higher in the *Myod1* transactivation group than the transgenic MYOD1 overexpression group ($p < 0.0001$). Expression of *Myog* ($p = 0.3740$) and *Desmin* ($p = 0.6588$) is similar in both the groups (two-way ANOVA, $n = 3$). Fold change in expression is relative to the (−) gRNA (−) MYOD1 transgene group.

(D) The effect of duration of reprogramming system induction by doxycycline on myogenic marker expression dynamics in C3H10T1/2 cells detected by qRT-PCR on day 18 posttransduction. The endogenous *Myod1* and *Myog* expression is significantly higher in the *Myod1* transactivation group than the transgenic MYOD1 overexpression group ($p < 0.0001$). Expression of *Desmin* ($p = 0.5348$) is similar in both the groups (two-way ANOVA, Bonferroni post tests, $n = 3$). Fold change in expression is relative to the (−) gRNA (−) MYOD1 transgene control group.

(E) Percentage of 4′,6-diamidino-2-phenylindole-stained nuclei that also express MYOD1/ MYOG protein in C3H10T1/2 cells on day 18 posttransduction is higher in the *Myod1* transactivation group (mean = ~34% MYOD1+, 33% MYOG+) than the MYOD1 overexpression group (mean = ~10% MYOD1+, 11% MYOG+) ($p = 0.0004$ [MYOD1], <0.0001 [MYOG], two-tailed unpaired t test, $n = 3$ biological replicates). Doxycycline induction of VdC9BV and MYOD1 transgenes was carried out for 8 days till day 10 posttransduction.

Data from independent biological replicates for (B)–(E) are represented as mean ± SEM.

process, endogenous *Myod1* expression over the entire duration was significantly higher in the ^{VP64}dCas9-BFP^{VP64}/gRNA-mediated activation group than the transgenic MYOD1 overexpression group. Expression kinetics of *Myog* and *Desmin* were similar in both the groups (Figure 4C).

The effects of limiting the activation of the ^{VP64}dCas9-BFP^{VP64}/gRNA system (by varying the duration of doxycycline exposure) on myogenic gene expression were compared with the MYOD1 overexpression system. Results showed that even a single day of doxycycline exposure (from day 2 to day 3 posttransduction) was adequate to activate the downstream myogenic genes (*Myog* and *Desmin*) to similar levels in both the groups and similar to levels achieved after 8 days of induction (Figure 4D). Almost all the markers on day 18 posttransduction after a maximum 8 days of induction had similar expression levels in both the groups (Figures 4D and S4A). However, both *Myod1* expression and the percentage of MYOD1 TF$^+$ nuclei were approximately 3-fold higher in the *Myod1* transactivation group than the MYOD1 overexpression group (Figures 4D, 4E, and S4B). It indicates that the higher expression of *Myod1* on quantitative RT-PCR (qRT-PCR) was probably a result of more MYOD1 TF$^+$ cells rather than higher expression levels in individual cells. *Myog* expression in C3H10T1/2 followed a pattern similar to *Myod1* (Figures 4D and 4E). Similar differential *Myod1* expression was also observed in the reprogrammed MEFs. However, expression of all the other myogenic markers and the percentage of MYOG$^+$ nuclei were similar in both groups (Figures S4C and S4D). It may be speculated that ^{VP64}dCas9-BFP^{VP64}/gRNA action renders the endogenous *Myod1* locus more receptive to MYOD1 TF-positive feedback response (Zingg et al., 1994). However, other cellular factors needed in conjunction with MYOD1 TF to initiate skeletal reprogramming may not be present in adequate quantities, thereby explaining the lack of a significant difference for other downstream late myogenic genes.

This study shows that the dual fusion of the VP64 transactivation domain to both the N and C terminus of dCas9 enables a high level of endogenous *Myod1* activation for the direct conversion of primary murine fibroblasts into SkMs. This potentiation of the transactivation process can be explained by an increased probability of the TFs homing onto two VP64 domains compared with just one VP64 domain. As a result, transcription can be initiated more frequently in the presence of ^{VP64}dCas9-BFP^{VP64}. Moreover, a synergistic transactivation effect resulting from favorable interactions of the TF complexes assembled on both the terminus of ^{VP64}dCas9-BFP^{VP64} can also help in explaining its potency. Improved nuclear localization of dCas9 afforded by increasing the number of NLS sequences, efficient lentiviral transgene delivery, inclusion of a BFP spacer sequence to decrease steric hindrance, and the identification of an efficient gRNA together complemented the effect of an additional VP64 domain in ^{VP64}dCas9-BFP^{VP64} to efficiently transactivate the endogenous *Myod1* locus. The results also demonstrate that CRISPR/Cas9-based transactivation performs comparably to the traditional MYOD1 overexpression-based skeletal reprogramming in upregulating some major myogenic genes. It augurs well for the potential use of this tool in reprogramming protocols that require complex and multiple TF activation.

In conclusion, we expect that this ^{VP64}dCas9-BFP^{VP64} platform, which is significantly more potent than previous versions, will encourage the adoption of CRISRP/Cas9-based TF technology to achieve multiplexed gene activation for reprogramming as well as nonreprogramming applications in basic science, biotechnology, and medicine.

EXPERIMENTAL PROCEDURES

gRNA Design

The gRNAs were designed by utilizing UCSC genome browser tracks (Feng Zhang Lab, MIT). The mouse *Myod1* locus-specific gRNAs 1–3 were selected to represent specific locations at a decreasing distance from the designated *Myod1* transcription initiation site, respectively. gRNA4 was selected to target the genome in the immediate vicinity of gRNA3, albeit on the opposite strand (Figure S1D). The human gRNA was picked to target the genome within 200 bases upstream of the *MYOD1* transcription initiation site.

^{VP64}dCas9-BFP^{VP64} Plasmid Construction

pdCas9::BFP-humanized plasmid (Addgene plasmid 44247) was used as the source of the dCas9-BFP fusion cassette. gBlock DNA fragments (Integrated DNA Technologies) were utilized to generate the ^{VP64}dCas9-BFP^{VP64} construct from dCas9-BFP and subsequently cloned into a lentiviral vector.

Cell Culture, Transfection, and Viral Transduction

All of the cell types used in this study were initially cultured with a high serum media (10% fetal bovine serum in Dulbecco's modified Eagle's medium-high glucose [DMEM-HG]). The cells were seeded at a density of 25,000 per well of a 12-well plate for transfection or transduction with components of the reprogramming system. Liposome-based transfection and lentiviral transduction were done while maintaining a constant dosage among the tests and controls. Low serum medium (2% horse serum in DMEM-HG) was used to induce skeletal differentiation.

Cell Staining and qRT-PCR

Four percent paraformaldehyde fixed cells were permeabilized with 0.2% Triton X-100 and subsequently stained with primary antibodies and fluorescent-labeled secondary antibodies. Relative quantification of gene expression (*delta-delta Ct method)* was performed on the RT-PCR data obtained by using SYBR green chemistry.

Statistical Analysis

Statistical analysis was done by GraphPad Prism 5.0 software. The convention followed to denote significance: *$p \leq 0.05$, **$p \leq 0.01$, and ***$p \leq 0.001$.

SUPPLEMENTAL INFORMATION

Supplemental Information includes Supplemental Experimental Procedures, four figures, and one movie and can be found with this article online at http://dx.doi.org/10.1016/j.stemcr.2014.09.013.

ACKNOWLEDGMENTS

Support from NIH (K.W.L.: EB015300, AI096305, UH2TR000505; C.A.G.: DP2OD008586, R01DA036865), National Science Foundation (CBET-1151035), American Heart Association (10SDG3060033), and the Muscular Dystrophy Association (MDA277360) is acknowledged. N.C. was supported by the Flight Attendant Medical Research Institute. We thank Pablo Perez-Pinera for helpful discussions. We also acknowledge Stanley Qi, Marius Wernig, and David Baltimore for Addgene plasmids 44247, 27152, and 14883, respectively. C.A.G. is an inventor on patent applications related to genome engineering and a scientific advisor to Editas Medicine.

Received: March 27, 2014
Revised: September 16, 2014
Accepted: September 17, 2014
Published: October 23, 2014

REFERENCES

Bikard, D., Jiang, W., Samai, P., Hochschild, A., Zhang, F., and Marraffini, L.A. (2013). Programmable repression and activation of bacterial gene expression using an engineered CRISPR-Cas system. Nucleic Acids Res. *41*, 7429–7437.

Cheng, A.W., Wang, H., Yang, H., Shi, L., Katz, Y., Theunissen, T.W., Rangarajan, S., Shivalila, C.S., Dadon, D.B., and Jaenisch, R. (2013). Multiplexed activation of endogenous genes by CRISPR-on, an RNA-guided transcriptional activator system. Cell Res. *23*, 1163–1171.

Cho, S.W., Kim, S., Kim, J.M., and Kim, J.S. (2013). Targeted genome engineering in human cells with the Cas9 RNA-guided endonuclease. Nat. Biotechnol. *31*, 230–232.

Cong, L., Ran, F.A., Cox, D., Lin, S., Barretto, R., Habib, N., Hsu, P.D., Wu, X., Jiang, W., Marraffini, L.A., and Zhang, F. (2013). Multiplex genome engineering using CRISPR/Cas systems. Science *339*, 819–823.

Davis, R.L., Weintraub, H., and Lassar, A.B. (1987). Expression of a single transfected cDNA converts fibroblasts to myoblasts. Cell *51*, 987–1000.

Farzadfard, F., Perli, S.D., and Lu, T.K. (2013). Tunable and multifunctional eukaryotic transcription factors based on CRISPR/Cas. ACS Synth. Biol. *2*, 604–613.

Gao, X., Yang, J., Tsang, J.C., Ooi, J., Wu, D., and Liu, P. (2013). Reprogramming to pluripotency using designer TALE transcription factors targeting enhancers. Stem Cell Rev. *1*, 183–197.

Gilbert, L.A., Larson, M.H., Morsut, L., Liu, Z., Brar, G.A., Torres, S.E., Stern-Ginossar, N., Brandman, O., Whitehead, E.H., Doudna, J.A., et al. (2013). CRISPR-mediated modular RNA-guided regulation of transcription in eukaryotes. Cell *154*, 442–451.

Hwang, W.Y., Fu, Y., Reyon, D., Maeder, M.L., Tsai, S.Q., Sander, J.D., Peterson, R.T., Yeh, J.R., and Joung, J.K. (2013). Efficient genome editing in zebrafish using a CRISPR-Cas system. Nat. Biotechnol. *31*, 227–229.

Jinek, M., Chylinski, K., Fonfara, I., Hauer, M., Doudna, J.A., and Charpentier, E. (2012). A programmable dual-RNA-guided DNA endonuclease in adaptive bacterial immunity. Science *337*, 816–821.

Jinek, M., East, A., Cheng, A., Lin, S., Ma, E., and Doudna, J. (2013). RNA-programmed genome editing in human cells. eLife *2*, e00471.

Kabadi, A.M., Ousterout, D.G., Hilton, I.B., and Gersbach, C.A. (2014). Multiplex CRISPR/Cas9-based genome engineering from a single lentiviral vector. Nucleic Acids Res. Published online August 13, 2014. http://dx.doi.org/10.1093/nar/gku749.

Kearns, N.A., Genga, R.M., Enuameh, M.S., Garber, M., Wolfe, S.A., and Maehr, R. (2014). Cas9 effector-mediated regulation of transcription and differentiation in human pluripotent stem cells. Development *141*, 219–223.

Konermann, S., Brigham, M.D., Trevino, A.E., Hsu, P.D., Heidenreich, M., Cong, L., Platt, R.J., Scott, D.A., Church, G.M., and Zhang, F. (2013). Optical control of mammalian endogenous transcription and epigenetic states. Nature *500*, 472–476.

Maeder, M.L., Linder, S.J., Cascio, V.M., Fu, Y., Ho, Q.H., and Joung, J.K. (2013). CRISPR RNA-guided activation of endogenous human genes. Nat. Methods *10*, 977–979.

Mali, P., Aach, J., Stranges, P.B., Esvelt, K.M., Moosburner, M., Kosuri, S., Yang, L., and Church, G.M. (2013a). CAS9 transcriptional activators for target specificity screening and paired nickases for cooperative genome engineering. Nat. Biotechnol. *31*, 833–838.

Mali, P., Yang, L., Esvelt, K.M., Aach, J., Guell, M., DiCarlo, J.E., Norville, J.E., and Church, G.M. (2013b). RNA-guided human genome engineering via Cas9. Science *339*, 823–826.

Perez-Pinera, P., Kocak, D.D., Vockley, C.M., Adler, A.F., Kabadi, A.M., Polstein, L.R., Thakore, P.I., Glass, K.A., Ousterout, D.G., Leong, K.W., et al. (2013). RNA-guided gene activation by CRISPR-Cas9-based transcription factors. Nat. Methods *10*, 973–976.

Qi, L.S., Larson, M.H., Gilbert, L.A., Doudna, J.A., Weissman, J.S., Arkin, A.P., and Lim, W.A. (2013). Repurposing CRISPR as an RNA-guided platform for sequence-specific control of gene expression. Cell *152*, 1173–1183.

Takahashi, K., and Yamanaka, S. (2006). Induction of pluripotent stem cells from mouse embryonic and adult fibroblast cultures by defined factors. Cell *126*, 663–676.

Zingg, J.M., Pedraza-Alva, G., and Jost, J.P. (1994). MyoD1 promoter autoregulation is mediated by two proximal E-boxes. Nucleic Acids Res. *22*, 2234–2241.

Stem Cell Reports, Volume *3*

Supplemental Information

A CRISPR/Cas9-Based System for Reprogramming Cell Lineage Specification

Syandan Chakraborty, HaYeun Ji, Ami M. Kabadi, Charles A. Gersbach, Nicolas Christoforou, and Kam W. Leong

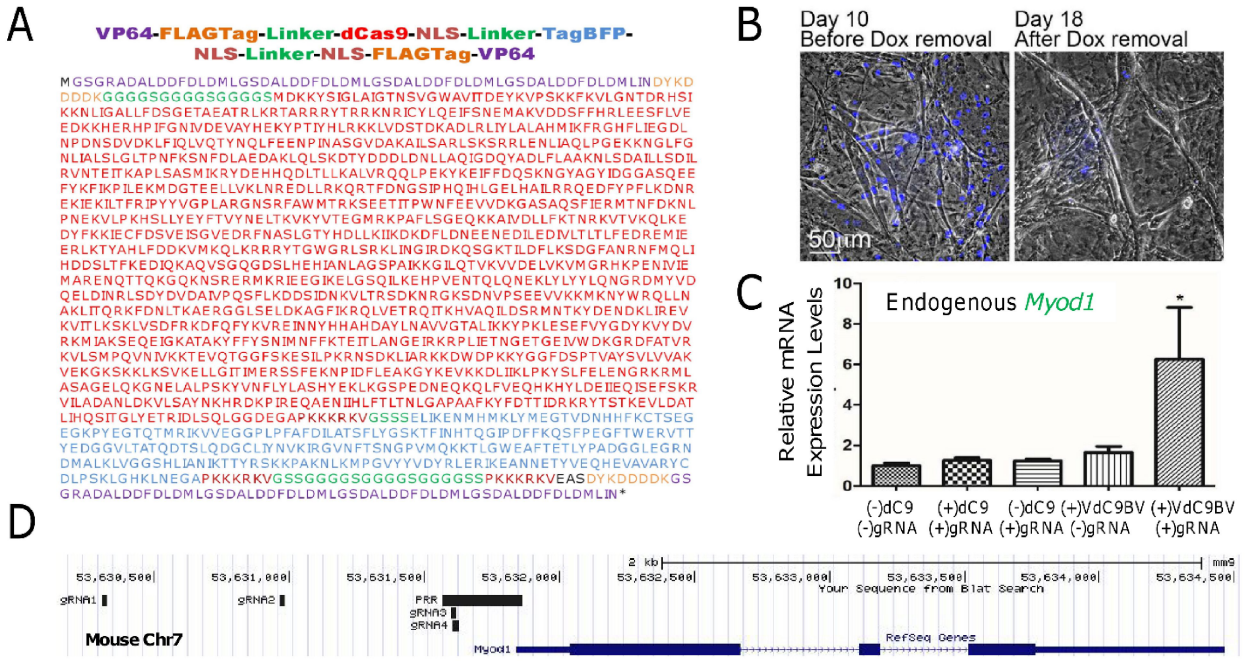

Figure S1: Supplemental Figure 1, related to Figure 1. Transactivation of the endogenous *Myod1* gene by a RNA-guided, nuclease-inactive, doxycycline-inducible ^{VP64}dCas9-BFP^{VP64} (VdC9BV) fusion protein.

(A) Amino acid sequence of the ^{VP64}dCas9-BFP^{VP64} fusion protein. **(B)** Doxycycline-inducible ^{VP64}dCas9-BFP^{VP64} expression. Following doxycycline addition to the culture medium, BFP is detected in the nuclei of multinucleated myotubes formed from reprogramming C3H10T1/2 cells. On removal of doxycycline most of the nuclei lose BFP expression. **(C)** ^{VP64}dCas9-BFP^{VP64} (VdC9BV) needs a gRNA to activate the endogenous *Myod1* gene. VdC9BV or gRNA alone cannot activate the gene. The VP64 fusion is needed for activation as gRNA+dCas9 cannot activate the gene. The studies were done by transfecting murine cell line C3H10T1/2. Control group = Mock transfection, (-) dC9 and (-) gRNA. (n=3 biological replicates, One Way ANOVA with Dunnett's Multiple Comparison Test with all groups compared to the Control, P<.05). Fold change in

expression is relative to the control group. **(D)** Mouse *Myod1* locus-specific gRNAs #1 - #4 represented in relation to the *Myod1* gene on Chromosome 7 and its proximal regulatory region (PRR, -275 to +20 relative to transcription start site). The representation has been done using UCSC genome browser BLAT search tool.

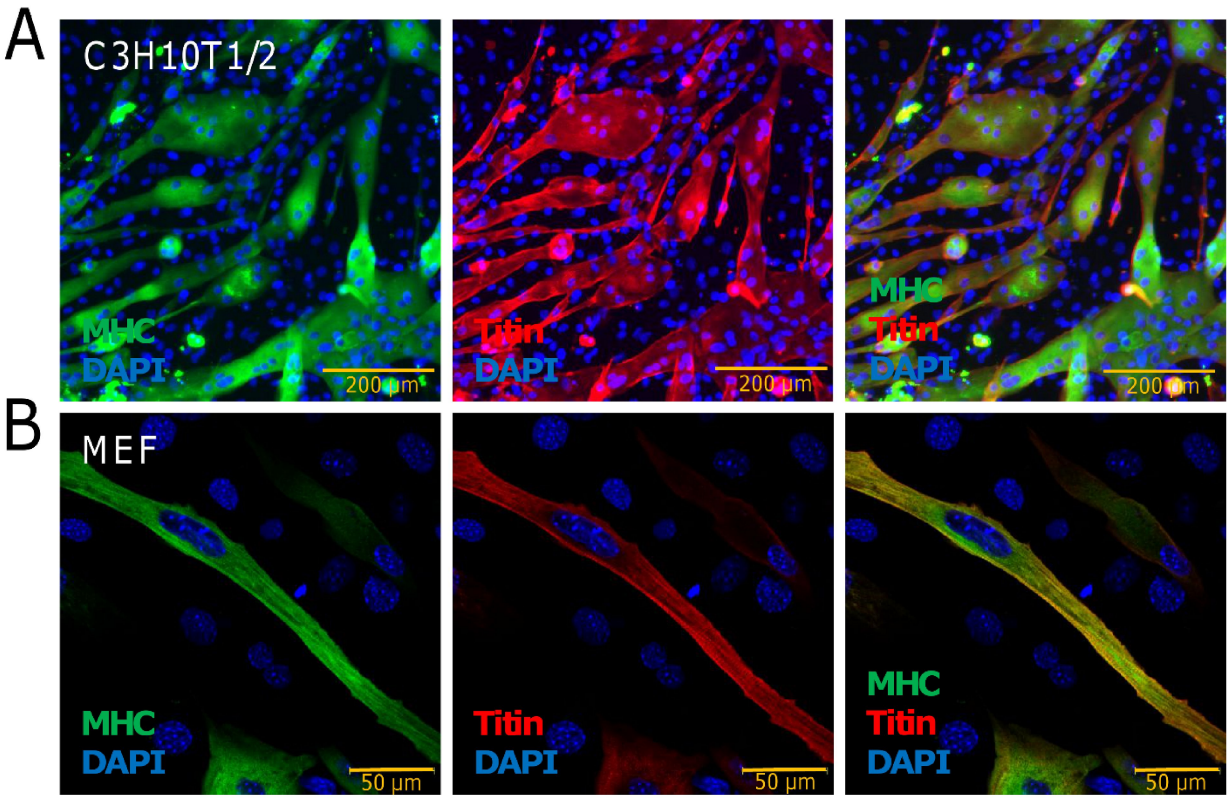

Figure S2: Supplemental Figure 2, related to Figure 2. Immunocytochemistry (ICC) staining of reprogrammed C3H10T1/2 cells and mouse embryonic fibroblasts (MEFs) for additional myogenic markers.

(A) Immunofluorescence microscopic imaging of reprogrammed C3H10T1/2 cells showing multinucleated myotubes characterized by the presence of sarcomeric proteins Myosin heavy chain (MHC) and Titin. **(B)** Confocal imaging of reprogrammed MEFs showing the emergence of cross-striated organization of sarcomeric Myosin heavy chain and Titin.

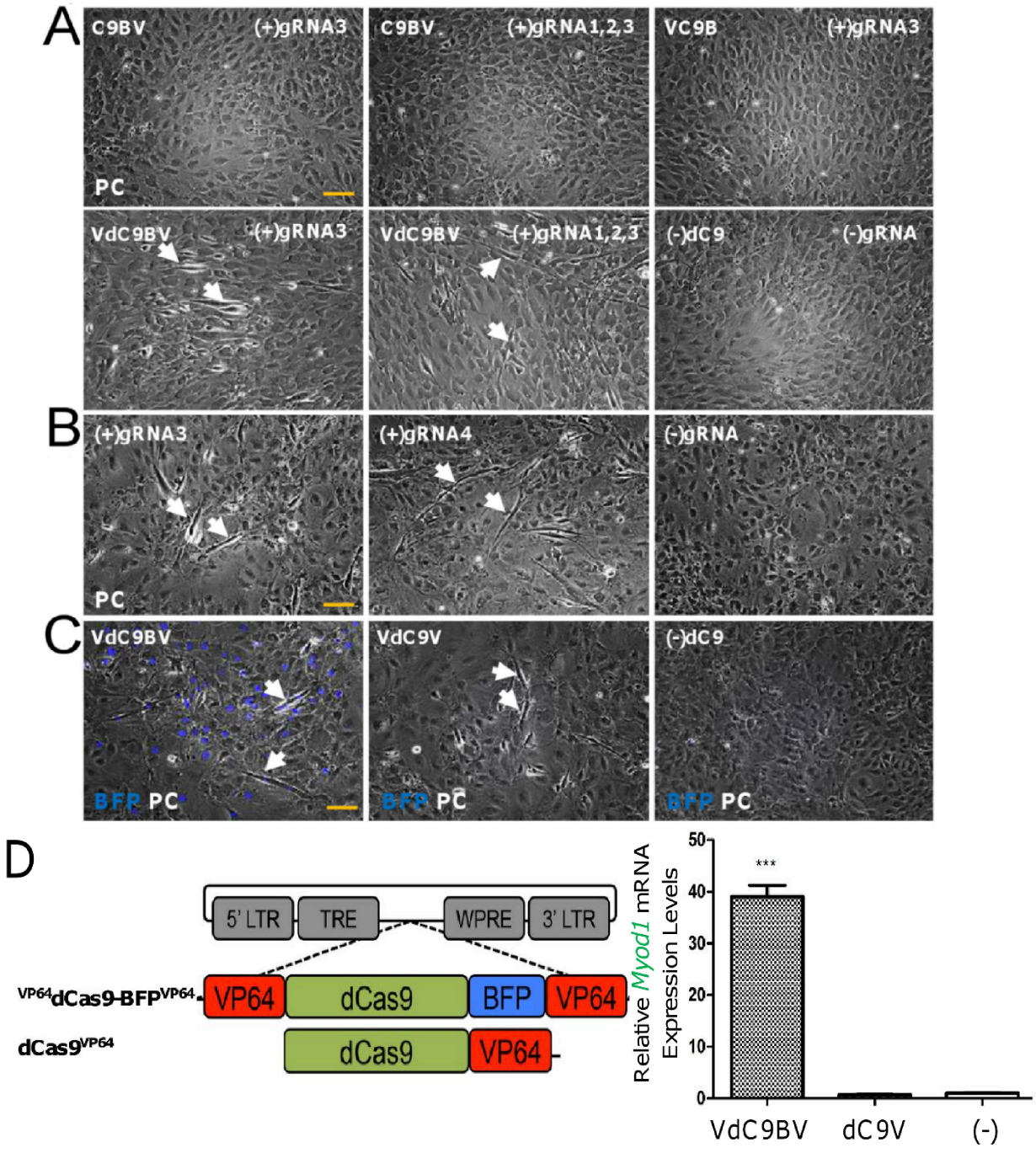

Figure S3: Supplemental Figure 3, related to Figure 3. Characteristics of gRNA-guided ^{VP64}dCas9-BFP^{VP64} (VdC9BV)-mediated activation of the endogenous *Myod1* gene locus.

(A) C-terminal-only and N-terminal-only VP64 fusion with dCas9-BFP cannot reprogram C3H10T1/2 cells into skeletal myocytes. Only VP64 fused to both N- and C-terminus of dCas9 can activate the endogenous *Myod1* gene sufficiently for myotube formation. The cells were imaged for the presence of developing myotubes (indicated by white arrows) which indicates initiation of reprogramming. Scale bar = 100μm. **(B)** gRNA4, designed with target sequence on the antisense strand, is able to trigger reprogramming in conjunction with VdC9BV similar to gRNA3 that targets the sense strand. The cells were imaged for the presence of developing myotubes (indicated by white arrows) which indicates initiation of reprogramming. Scale bar = 100μm. **(C)** Both BFP-fused and -unfused forms of VdC9BV transgene can activate the endogenous *Myod1* gene for skeletal reprogramming. The cells were imaged for the presence of developing myotubes (indicated by white arrows) which indicates initiation of reprogramming. Scale bar = 100μm. **(D)** Illustration depicting dCas9-based activators $^{\mathbf{VP64}}$dCas9-BFP$^{\mathbf{VP64}}$ (VdC9BV) and dCas9$^{\mathbf{VP64}}$ (dC9V) and qRT.PCR analysis showing failure of the C-terminal VP64 fusion to dCas9 (dCas9$^{\mathbf{VP64}}$, a BFP-less form) to activate the *Myod1* locus of C3H10T1/2 cells ($P \leq .001$, One-way ANOVA, Dunnett's post hoc test, n=3 biological replicates). All the experiments **(A-D)** were done in C3H10T1/2 cells. Images were acquired at six days post-transduction.

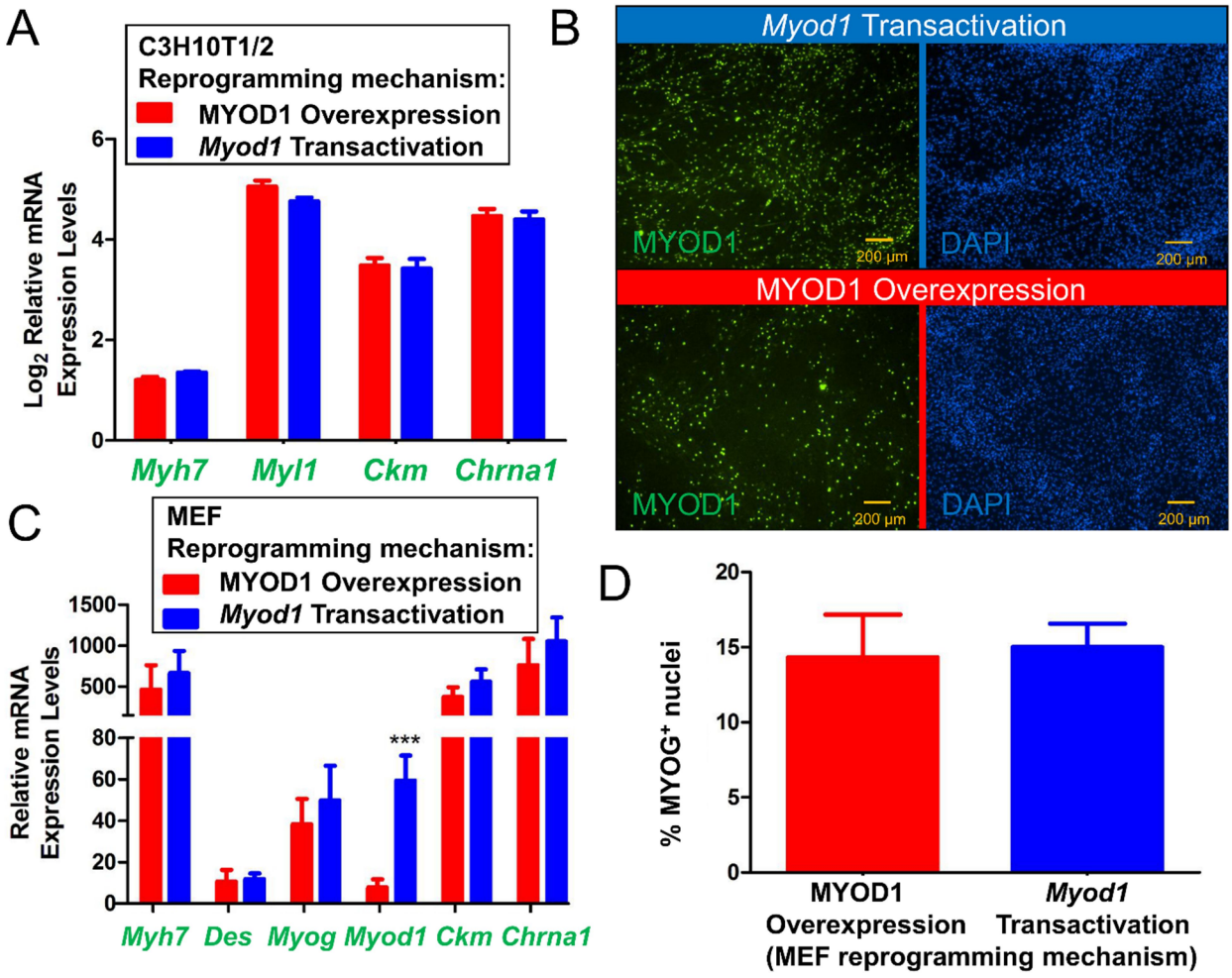

Figure S4: Supplemental Figure 4, related to Figure 4. Comparison of skeletal reprogramming by gRNA-guided ^{VP64}dCas9-BFP^{VP64} (VdC9BV)-mediated transactivation of the endogenous *Myod1* gene locus and by transgenic MYOD1 overexpression.

(A) Expression of myogenic markers in C3H10T1/2s (detected by qRT.PCR) on day 18 post-transduction by VdC9BV-mediated transactivation of the endogenous *Myod1* gene is similar to that activated by transgenic MYOD1 overexpression (comparison of individual markers was done by one-way ANOVA with Bonferroni post tests, n=3 biological replicates, error bars=SEM). Fold change in expression is relative to the (-) gRNA (-)

MYOD1 transgene control group. Doxycycline induction of VdC9BV and MYOD1 transgenes was carried out for 8 days till day 10 post-transduction. **(B)** Percentage of DAPI-stained nuclei that also express MYOD1 protein in C3H10T1/2s (detected by ICC) on day 18 post-transduction by transactivation of the endogenous *Myod1* gene is higher than that mediated by transgenic MYOD1 overexpression. **(C)** Expression of myogenic markers in mouse embryonic fibroblasts (detected by qRT.PCR) on day 22 post-transduction by transactivation of the endogenous *Myod1* gene is similar ($P>.05$) to that mediated by transgenic MYOD1 overexpression except for the expression of *Myod1* mRNA ($P\leq.001$) (comparison of individual markers was done by one-way ANOVA with Bonferroni post tests, n=3 biological replicates, Error bars=SEM). Fold change in expression is relative to the (-) gRNA (-) MYOD1 transgene control group. The doxycycline induction of VdC9BV and MYOD1 transgenes was carried out for 10 days till day 12 post-transduction. **(D)** Percentage of DAPI-stained nuclei that also express MYOG in mouse embryonic fibroblasts (detected by ImageJ-aided counting from ICC images) on day 22 post-transduction in the *Myod1* gene transactivation group (mean=~15%) is statistically similar to that mediated by transgenic MYOD1 overexpression (mean=~14.5%) (Two-tailed unpaired t test, n=3 biological replicates, Error bars=SEM).

Movie S1: Supplemental Movie S1, related to Figure 1. Video showing spontaneous twitching of skeletal myocytes reprogrammed from mouse embryonic fibroblast on post transduction day 22.

Supplemental Experimental Procedures

Guide RNA plasmid construction. Ubiquitin promoter-driven Green Fluorescent Protein cassette was removed from FUGW plasmid (Addgene plasmid 14883) by digesting with PacI and XhoI. For expressing a chimeric gRNA from the human U6 promoter a gBlock fragment (Integrated DNA Technologies, Inc., USA) was synthesized (Mali et al., 2013). It incorporated a BsmBI site, distal to the U6 promoter, for easy incorporation of new gRNA spacer sequences. The gBlock was then cloned into the restriction-digested FUGW backbone (Figure 1C). For targeting 23bp sequences in the genome of the form $NNNNNNNNNNNNNNNNNNNN_{(N=20)}$-$NGG_{(PAM)}$, plus and minus strand DNA oligos were designed to contain the protospacer sequence. An overhang was produced after annealing of the oligos that was complementary to the overhangs created in the vector after digestion with BsmBI. After ligation, the gRNA expression plasmids were subsequently packaged in lentiviral vectors.

The following gRNA-targeted sites were used in the study:

Mouse *Myod1* (*Myod1* Transcript Position: chr7:53,631,844-53,634,462) gRNA-targeted sequence:

gRNA1(+strand chr7:53630309-53630328): GTATCAGAGACAAAAACCGT;

gRNA2(-strand chr7:53630967-53630986): TTCTTAAGGATCGTGATGGC;

gRNA3(+strand chr7:53631602-53631621): TAGCCAAGTGCTACCGCGTA;

gRNA4(-strand chr7:53631608-53631627): CAGCCATACGCGGTAGCACT.

Human *MYOD1* (*MYOD1* Transcript Position: chr11:17,741,110-17,743,678) gRNA-targeted sequence:

(+strand chr11:17740919-17740938): ACCTAGCGCGCACGCCAGTG.

^{VP64}dCas9-BFP^{VP64} plasmid construction. The dCas9-BFP fusion cassette was digested from the pdCas9::BFP-humanized plasmid (Addgene plasmid 44247). Two gBlock DNA fragments were synthesized: one having the N-terminal VP64, FLAG tag, and linker sequence and the other having the C-terminal VP64 along with a FLAG tag, an additional nuclear localization signal, and a linker sequence. The lentiviral backbone along with the doxycycline inducible promoter was derived from Tet-O-FUW-Myt1l (Addgene plasmid 27152) (Vierbuchen et al., 2010). All four fragments were digested to generate compatible sticky ends. All the digested fragments were then joined together by a four-way ligation reaction to form TetO-FUW-^{VP64}dCas9-BFP^{VP64} (Figure 1C). The final amino acid sequence of the construct is provided in Supplemental Figure 1A. This plasmid was used to produce all the other forms including N-terminal-only VP64, C-terminal-only VP64, and the BFP-deleted fusion construct. Q5 High Fidelity DNA polymerase (New England Biolabs. MA, USA) along with corresponding primers were used to PCR amplify the required fragments to be ligated back into the doxycycline inducible viral backbone to generate all the other forms mentioned above. A doxycycline inducible form of MYOD1 was also generated by inserting a human *MYOD1* element (LIFESEQ3292930, Open Biosystems) into the same lentiviral plasmid backbone.

Cell culture, transfection and viral transduction. Primary mouse embryonic fibroblasts (PMEF) (Lonza), human embryonic kidney 293T cells (HEK 293T) (ATCC) and C3H10T1/2 cells (ATCC) were utilized in this study. All the cell types were initially cultured with 10% fetal bovine serum (FBS) (Atlanta Biologicals) in DMEM-HG (GIBCO-11960) supplemented with L-glutamine, pyruvate and MEM-NEAA (GIBCO). The HEK293Ts were utilized for lentivirus generation and for verifying the efficacy of ^{VP64}dCas9-BFP^{VP64}

to transactivate the endogenous human *MYOD1* locus. The other two cell types were utilized in reprogramming studies. For reprogramming the cells were seeded at a density of 25,000/well of a 12-well plate. Transfection of C3H10T1/2 was done by using Lipofectamine LTX with plus reagent (Life Technologies). Cells were transfected at a confluency of 70%. 2 µg of plasmid DNA was delivered to each well of a 12-well plate at a ratio of 4:1:1 (^{VP64}dCas9-BFP^{VP64}:M2rtTA:U6-gRNA). For transduction, the lentiviruses were added at a total MOI (multiplicity of infection) of 60: ^{VP64}dCas9-BFP^{VP64}=MOI of 40, M2rtTA=MOI of 10, U6-gRNA=MOI of 10. For the experimental controls, empty FUW lentiviral backbone (Ubiquitin C promoter removed from the FUW lentiviral construct) was transduced to maintain the total MOI (Figure 1C). To improve transduction, Sequebrene was added to the medium at a concentration of 8 µg/ml. Doxycycline at a concentration of 3 µg/ml was added to cultures on day 2 post transduction. In the case of C3H10T1/2 cells, doxycycline induction was continued till day 10 in a low serum differentiation media composed of 2% Horse Serum (Sigma Aldrich) in DMEM-HG (GIBCO-11960) supplemented with L-glutamine, pyruvate and MEM-NEAA (GIBCO). Subsequently the media was switched to a doxycycline-free low serum media. On day 18 post-transduction the cells were fixed and stained and RNA was extracted for RT.PCR. For the PMEFs, doxycycline was continued till day 12 and subsequently switched to a no-doxycycline medium till day 22. For PMEFs the differentiation media had 10% FBS till day 12 and subsequently changed to 2% FBS (Figure 2E).

Lentiviral production. Lentiviral particles were produced by transfecting HEK 293T cells with the transfer plasmid (TetO-FUW-^{VP64}dCas9-BFP^{VP64}, TetO-FUW-dCas9-BFP^{VP64}, TetO-FUW-^{VP64}dCas9-BFP, TetO-FUW-^{VP64}dCas9^{VP64}, U6-gRNA, FUW-M2rtTA, Empty

FUW) along with 2nd generation packaging plasmids (Addgene plasmid 12260: psPAX2 and Addgene plasmid 12259: pMD2.G). The procedure for lentivirus generation and extraction has been described elsewhere (Chakraborty et al., 2013). For determining the titer of the lentivirus, a qRT.PCR-based lentiviral titration kit was used according to the manufacturer's instructions (Applied Biological Materials Inc., Richmond, Canada).

Quantitative real time reverse-transcription polymerase chain reaction (qRT.PCR) and reverse-transcription polymerase chain reaction (RT.PCR). The primers were purchased from IDT (Coralville, Iowa). Total RNA was extracted with a Clontech RNA clean-up kit. cDNA was generated by iScript cDNA Synthesis kit (Bio-Rad). PCR was done by utilizing *Taq* DNA Polymerase with ThermoPol® Buffer (NEB). The cycling conditions were: Activation: 95°C for 30 sec; Denaturation: 95°C for 20 sec, Annealing: 58°C for 30 sec, Extension: 68°C for 60 sec, for varying number of cycles; Final Extension: 72°C for 5 min. For qRT.PCR, SsoAdvanced™ Universal SYBR® Green Supermix from Bio-Rad was used according to the manufacturer's instruction. The expression levels are presented as fold change relative to a control group (*delta-delta Ct method).* GAPDH was used as the housekeeping endogenous control gene to normalize target gene expression.

Primer sequences for quantitative real time reverse-transcription polymerase chain reaction (qRT.PCR) and reverse-transcription polymerase chain reaction (RT.PCR). The following primers were utilized in this study:

dCas9: AGGGATTAAGGAGCTCGGGT, AGGAAGCTCTGAGGGACGAT;

Mu-*Myod1*: AGCGACACAGAACAGGGAAC, TCGAAAGGACAGTTGGGAAG;

Mu-*Myog*: GAGACATCCCCCTATTTCTACCA, GCTCAGTCCGCTCATAGCC;

Mu-*Desmin*: GTGGATGCAGCCACTCTAGC, TTAGCCGCGATGGTCTCATAC;

Mu-*Myl1*: AAGATCGAGTTCTCTAAGGAGCA, TCATGGGCAGAAACTGTTCAAA;

Mu *Ckm*: CTGACCCCTGACCTCTACAAT, CATGGCGGTCCTGGATGAT;

Mu-*Chrna1*: GCACCTGGACCTATGACGGC, TAAGACAGAGATGCTCAGCG;

Mu-*Myh7*: CTCAAGCTGCTCAGCAATCTATTT, GGAGCGCAAGTTTGTCATAAGT;

Mu-*Gapdh*: TGCGACTTCAACAGCAACTC, CTTGCTCAGTGTCCTTGCTG;

Hu-*MYOD1*: CTTTGCTATCTACAGCCGGG, GAGTGCTCTTCGGGTTTCAG;

Transgenic Hu-MYOD1: CGGCATGATGGACTACAGCG,

CAGGCAGTCTAGGCTCGAC;

Hu-*GAPDH*: GGAGCGAGATCCCTCCAAAAT, GGCTGTTGTCATACTTCTCATGG.

Cell fusion assay. C3H10T1/2 cells were sequentially transduced with TetO-FUW-^{VP64}dCas9-BFP^{VP64} and M2rtTA virus. This cell population was subsequently divided and transduced with either LV-CRE or LV-Floxed Luc. These cell populations were mixed and plated in a 1:1 ratio of LV-CRE transduced cells to LV- Floxed Luc cells and transduced with the *Myod1* gRNA virus. The cells were induced to express ^{VP64}dCas9-BFP^{VP64} by adding 3 µg/ml doxycycline to the medium on day 6 post-transduction with ^{VP64}dCas9-BFP^{VP64}. Medium containing fresh doxycycline was replenished every two days for the next eight days. Subsequently doxycycline was withdrawn on day 14 post-transduction with ^{VP64}dCas9-BFP^{VP64}. Fresh medium without doxycycline was then replenished every two days. Samples were harvested on day 14 and day 22 and assayed for luciferase expression. Briefly, cells were pelleted and washed with PBS. Pellets were re-suspended in 100 µL of lysis buffer (100mM KH2PO4 + 0.2% Triton-X, pH 7.8) and incubated at room temperature for 10 min. The cell debris was pelleted and 30 µl of the supernatant from each sample was transferred to an opaque 96-well plate. Each sample was mixed with

30 µL of Bright-Glo reagent (Bright-Glo Luciferase Assay System, Promega). Luminescence was measured by a BioTek Synergy 2 Multi-Mode Microplate Reader with 1-second scan time. All luciferase data is presented as a fold increase over background of samples transduced with VP64dCas9-BFPVP64, M2rtTA, and LV-Floxed Luc (Figure 2D).

Cell staining, imaging, analysis and illustrations. The cells were then stained with primary antibodies against: Desmin (Monoclonal Anti-Pig Desmin, mouse IgG1 isotype, Sigma Aldrich, D1033), MYOD1 (Monoclonal Anti-Mouse MYOD1, mouse IgG1 isotype, Pierce, MA141017), Myogenin (Monoclonal Anti-Rat Myogenin, mouse IgG1 isotype, Developmental Studies Hybridoma Bank, F5D), FLAG™ Epitope Tag (Mouse monoclonal IgG2b, Pierce, MA1-91878), F-Actin (Alexa Fluor 594 Phalloidin, Life Technologies, A12381), α-Actinin (Monoclonal Anti-Rabbit Skeletal α-Actinin, mouse IgG1 isotype, Sigma Aldrich, A7811), Myosin heavy chain (Monoclonal Anti-Chicken Sacrcomeric Myosin, mouse IgG2b isotype, Developmental Studies Hybridoma Bank, MF 20), Titin (Monoclonal Anti-Bovine Titin, mouse IgM isotype, Developmental Studies Hybridoma Bank, 9 D10). DAPI was used to stain the nucleus. Alexa Fluor 488 Goat Anti-mouse IgG, Alexa Fluor 568 Goat Anti-rabbit IgG and Alexa Fluor 568 Goat Anti-mouse IgM (Life technologies) were used as the secondary antibody for ICC. Fluorescent images were captured using Nikon Eclipse TE2000-U with a Roper Scientific CoolSnap HQ camera or Zeiss 510 inverted confocal microscope. Acquired images were displayed by using Nikon NIS Elements or Zeiss AIM LSM Image browser for the confocal images. ImageJ (http://rsb.info.nih.gov/ij) was used for counting the marker^{+} nuclei on the ICC images. Three fields were randomly chosen for each replicate. ImageJ was also used to manually

define the nuclear and the cytoplasmic regions on the images and to calculate the average fluorescence intensity. Illustrations were created by adapting templates from Servier Medical Arts (http://www.servier.com/Powerpoint-image-bank, licensed under a Creative Commons Attribution 3.0 Unported License).

Supplemental References

Chakraborty, S., Christoforou, N., Fattahi, A., Herzog, R.W., and Leong, K.W. (2013). A robust strategy for negative selection of Cre-loxP recombination-based excision of transgenes in induced pluripotent stem cells. PloS one *8*, e64342.
Mali, P., Yang, L., Esvelt, K.M., Aach, J., Guell, M., DiCarlo, J.E., Norville, J.E., and Church, G.M. (2013). RNA-guided human genome engineering via Cas9. Science *339*, 823-826.
Vierbuchen, T., Ostermeier, A., Pang, Z.P., Kokubu, Y., Sudhof, T.C., and Wernig, M. (2010). Direct conversion of fibroblasts to functional neurons by defined factors. Nature *463*, 1035-1041.